



**HAL**  
open science

## **AMPK activation induces immunogenic cell death in AML**

Johanna Mondesir, Margherita Ghisi, Laura Poillet, Robert Bossong, Oliver Kepp, Guido Kroemer, Jean-Emmanuel Sarry, Jérôme Tamburini, Andrew Lane

► **To cite this version:**

Johanna Mondesir, Margherita Ghisi, Laura Poillet, Robert Bossong, Oliver Kepp, et al.. AMPK activation induces immunogenic cell death in AML. *Blood Advances*, In press, 10.1182/bloodadvances.2022009444 . hal-04291063v1

**HAL Id: hal-04291063**

**<https://hal.science/hal-04291063v1>**

Submitted on 17 Nov 2023 (v1), last revised 15 Nov 2024 (v2)

**HAL** is a multi-disciplinary open access archive for the deposit and dissemination of scientific research documents, whether they are published or not. The documents may come from teaching and research institutions in France or abroad, or from public or private research centers.

L'archive ouverte pluridisciplinaire **HAL**, est destinée au dépôt et à la diffusion de documents scientifiques de niveau recherche, publiés ou non, émanant des établissements d'enseignement et de recherche français ou étrangers, des laboratoires publics ou privés.

## AMPK activation induces immunogenic cell death in AML

Tracking no: ADV-2022-009444R1

Johanna Mondesir (Dana-Farber Cancer Institute, Harvard Medical School, Institut Cochin, United States) Margherita Ghisi (CRCT, France) Laura Poillet (CRCT, France) Robert Bossong (Dana-Farber Cancer Institute, Harvard Medical School, United States) Oliver Kepp (INSERM UMR1138, France) Guido Kroemer (Cordeliers Research Center, INSERM U1138, France) Jean-Emmanuel Sarry (INSERM, France) Jérôme Tamburini (Geneva University, Switzerland) Andrew Lane (Dana-Farber Cancer Institute, Harvard Medical School, United States)

### Abstract:

Survival of patients with acute myeloid leukemia (AML) can be improved by allogeneic hematopoietic stem cell transplantation (alloHSCT) due to the anti-leukemic activity of T- and NK-cells from the donor. However, the use of alloHSCT is limited by donor availability, recipient age, and potential severe side effects. Similarly, the efficacy of immunotherapies directing autologous T-cells against tumor cells, including T-cell recruiting antibodies, chimeric antigen receptor T-cell therapy, and immune checkpoint inhibitors is limited in AML due to multiple mechanisms of leukemia immune escape. This has prompted a search for novel immunostimulatory approaches. Here, we show that activation of AMP-activated protein kinase (AMPK), a master regulator of cellular energy balance, by the small molecule GSK621 induces calreticulin (CALR) membrane exposure in murine and human AML cells. When CALR is exposed on the cell surface, it serves as a damage-associated molecular pattern (DAMP) that stimulates immune responses. We found that GSK621-treated murine leukemia cells promote the activation and maturation of bone marrow-derived dendritic cells. Moreover, vaccination with GSK621-treated leukemia cells had a protective effect in syngeneic immunocompetent recipients bearing transplanted AMLs. This effect was lost in recipients depleted of CD4/CD8 T cells. Together, these results demonstrate that AMPK activation by GSK621 elicits traits of immunogenic cell death and promotes a robust immune response against leukemia. Pharmacologic AMPK activation thus represents a new potential target for improving the activity of immunotherapy in AML.

**Conflict of interest:** COI declared - see note

**COI notes:** GK declares having held research contracts with Daiichi Sankyo, Eleor, Kaleido, Lytix Pharma, PharmaMar, Osasuna Therapeutics, Samsara Therapeutics, Sanofi, Sotio, Tollys, Vascage and Vasculox/Tioma, has received consulting/advisory honoraria from Reithera, is on the Board of Directors of the Bristol Myers Squibb Foundation France, is a scientific co-founder of everImmune, Osasuna Therapeutics, Samsara Therapeutics and Therafast Bio, and is the inventor of patents covering therapeutic targeting of aging, cancer, cystic fibrosis and metabolic disorders. AAL has received research funding from AbbVie and Stemline Therapeutics, and consulting fees from Adaptimmune, Cimeio, IDRx, N-of-one, Qiagen, and Stemline Therapeutics.

**Preprint server:** No;

**Author contributions and disclosures:** JM: conceptualization, resources, data curation, data analysis, supervision, funding acquisition, validation, investigation, methodology, writing-original draft; MG, LP: resources, data analysis, investigation, methodology; RAB: investigation; OK, GK: methodology; JES: resources, methodology; JT, AAL: conceptualization, resources, supervision, funding acquisition, writing-review and editing.

**Non-author contributions and disclosures:** No;

**Agreement to Share Publication-Related Data and Data Sharing Statement:** Data may be shared by contacting the corresponding author.

Clinical trial registration information (if any):

# AMPK activation induces immunogenic cell death in AML

Johanna Mondesir<sup>1,2</sup>, Margherita Ghisi<sup>3,4,5,#</sup>, Laura Poillet<sup>3,4,5,#</sup>, Robert A. Bossong<sup>1</sup>, Oliver Kepp<sup>6,7</sup>, Guido Kroemer<sup>6,7,8</sup>, Jean-Emmanuel Sarry<sup>3,4,5</sup>, Jérôme Tamburini<sup>2,9,10,11,§</sup>, and Andrew A. Lane<sup>1,§</sup>

<sup>1</sup> Department of Medical Oncology, Dana-Farber Cancer Institute, Harvard Medical School, Boston, MA

<sup>2</sup> Université de Paris, Institut Cochin, CNRS UMR8104, INSERM U1016, 75014 Paris, France

<sup>3</sup> Centre de Recherches en Cancérologie de Toulouse, Inserm U1037, CNRS U5071, Université de Toulouse, Toulouse, France.

<sup>4</sup> LabEx Toucan, Toulouse, France.

<sup>5</sup> Équipe labellisée Ligue contre le cancer 2023, Toulouse, France.

<sup>6</sup> Equipe labellisée Ligue contre le cancer, Université de Paris Cité, Sorbonne Université, INSERM UMR1138, Centre de Recherche des Cordeliers, Paris, France

<sup>7</sup> Metabolomics and Cell Biology Platforms, Gustave Roussy, Villejuif, France

<sup>8</sup> Institut du Cancer Paris CARPEM, Department of Biology, Hôpital Européen Georges Pompidou, AP-HP, Paris, 75015, France

<sup>9</sup> Equipes Labellisées Ligue Nationale Contre le Cancer (LNCC), Paris, France

<sup>10</sup> Translational Research Centre in Onco-hematology, Faculty of Medicine, University of Geneva, 1211 Geneva, Switzerland

<sup>11</sup> Swiss Cancer Center Leman, Lausanne, Switzerland

#Contributed equally

§Contributed equally

Correspondence:

Andrew A. Lane, MD, PhD  
Dana-Farber Cancer Institute  
450 Brookline Ave, Mayer 413  
Boston, MA 02215  
[andrew\\_lane@dfci.harvard.edu](mailto:andrew_lane@dfci.harvard.edu)

Short title: AML immunogenic cell death by AMPK activation

Figures: 4

Supplementary Figures: 4

Supplementary Table: 1

Abstract word count: 230

Text word count: 4130

References: 42

## Abstract

Survival of patients with acute myeloid leukemia (AML) can be improved by allogeneic hematopoietic stem cell transplantation (alloHSCT) due to the anti-leukemic activity of T- and NK-cells from the donor. However, the use of alloHSCT is limited by donor availability, recipient age, and potential severe side effects. Similarly, the efficacy of immunotherapies directing autologous T-cells against tumor cells, including T-cell recruiting antibodies, chimeric antigen receptor T-cell therapy, and immune checkpoint inhibitors is limited in AML due to multiple mechanisms of leukemia immune escape. This has prompted a search for novel immunostimulatory approaches. Here, we show that activation of AMP-activated protein kinase (AMPK), a master regulator of cellular energy balance, by the small molecule GSK621 induces calreticulin (CALR) membrane exposure in murine and human AML cells. When CALR is exposed on the cell surface, it serves as a damage-associated molecular pattern (DAMP) that stimulates immune responses. We found that GSK621-treated murine leukemia cells promote the activation and maturation of bone marrow-derived dendritic cells. Moreover, vaccination with GSK621-treated leukemia cells had a protective effect in syngeneic immunocompetent recipients bearing transplanted AMLs. This effect was lost in recipients depleted of CD4/CD8 T cells. Together, these results demonstrate that AMPK activation by GSK621 elicits traits of immunogenic cell death and promotes a robust immune response against leukemia. Pharmacologic AMPK activation thus represents a new potential target for improving the activity of immunotherapy in AML.

## Key Points

- AMPK activation by GSK621 enhances pre-apoptotic surface exposure of calreticulin in AML
- AML cells primed by AMPK activation are potent dendritic cell activators and induce anticancer immunity in vivo

## Introduction

Acute myeloid leukemia (AML) is an aggressive malignancy that arises from transformation of myeloid precursors. While chemotherapy remains a cornerstone for the treatment of AML, new agents targeting molecular dependencies, such as FLT3 or BCL2 inhibitors, are becoming available.<sup>1</sup> However, most patients still succumb to relapsed/refractory disease, demonstrating a need for new therapeutic strategies.

Immunotherapy in the form of allogeneic hematopoietic stem cell transplantation (alloHSCT) is widely employed to consolidate remission induced by cytotoxic agents in patients with AML. Nonetheless, major side effects including infections and graft-versus-host disease considerably limit the use of alloHSCT, especially in the elderly.<sup>2,3</sup> As the anti-leukemic effects of alloHSCT are mainly mediated by cellular immunity, new T-cell activating immunotherapies are actively being investigated in AML, such as T-cell engaging antibodies, chimeric antigen receptors (CAR), and immune checkpoint inhibitors (ICI).<sup>4</sup> Yet, anti-leukemic activity of these immunotherapies in AML appears to be modest, at least in studies to date.<sup>5</sup>

Amongst various modalities of cell death, immunogenic cell death (ICD) is relevant to cancer therapy because it promotes an anti-tumor immune response through tumor-specific antigenicity and adjuvanticity. This response is mediated by the release of damage-associated molecular patterns (DAMPs) that can activate dendritic cells (DCs) thus shaping the tumor immune microenvironment.<sup>6,7</sup> Cellular changes in response to environmental or internal signals are critical in the adjuvanticity of cells undergoing ICD, and the integrated stress response (ISR) pathway recently emerged as a hallmark of ICD.<sup>8</sup>

ISR pathways converge on phosphorylation of eukaryotic translation initiation factor 2 subunit alpha (eIF2 $\alpha$ ), which is also a characteristic feature of ICD.<sup>9</sup> Protein kinase RNA-like ER kinase

(PERK) is an eIF2 $\alpha$  kinase that participates in the endoplasmic reticulum (ER) stress response, which activates the transcription factor ATF4 involved in cell death and autophagy.<sup>10</sup> eIF2 $\alpha$  phosphorylation is required for exposure of the ER chaperone calreticulin (CALR) at the cell surface, which serves as an activating 'eat-me signal' for DCs.<sup>11</sup>

Using the selective AMP-activated protein kinase (AMPK) activator GSK621, we recently showed that AMPK elicits a stress response through PERK and ATF4 activation, leading to enhanced mitochondrial susceptibility of AML to the BCL2 inhibitor venetoclax.<sup>12</sup> As AMPK activation induces eIF2 $\alpha$  phosphorylation through PERK activation, we hypothesized that AMPK activation might also trigger ICD in AML.

Here, we tested this hypothesis and found that GSK621 induced multiple features of ICD in AML. These effects were AMPK-dependent, involved the activation of PERK, and were seen in human and mouse AML cells, including in immunocompetent syngeneic in vivo models of vaccination and tumor challenge. Together, our results show a new function of AMPK in regulating stress-induced ICD, suggesting the potential of AMPK activation to favor anti-leukemic immune activity.

## Methods

### Patient samples

Patient AML cells were from fresh or viably cryopreserved bone marrow aspirates collected at the time of diagnosis. All patients consented to an IRB approved banking protocol. Clinical details are in Supplementary Table 1.

### Cell lines

Murine C1498 cells were purchased from American Type Culture Collection (ATCC TIB-49) in 2018. Human AML cell lines were obtained from ATCC between 2009 and 2015, STR profiled periodically, and verified mycoplasma negative yearly. Cells were cultured at 37°C in 5% CO<sub>2</sub> with Minimum Essential Medium alpha (Gibco, 12561-072) supplemented with 10% fetal bovine serum (Sigma Aldrich, F2442), 1 mM L-alanyl-L-glutamine (Corning, 25-015-CI), and 100 U/100 µg/ml Penicillin/Streptomycin.

### Generation of CRISPR KO Cells

*Murine cells.* To generate controls for surface calreticulin flow cytometry, C1498 cell lines were retrovirally transduced with a pRetro\_*CALR*-DAF\_DsRed<sup>13</sup> or *Calr* was deleted by CRISPR-Cas9. Cells were transfected with lentivirus containing sgRNAs targeting *Calr* or a non-targeting guide. For murine AML cells on a transgenic Cas9 background (see below), sgRNAs were cloned in the lentiviral vector pLKO5.sgRNA.EFS.tRFP (Addgene #57823), cells were infected, and RFP positive cells were sorted. sgRNA sequences: *Calr* (sgRNA#1: TATGTTTGGATTTCGACCCAG; sgRNA#2: ATAGATGGCAGGGTCTGCGG; sgRNA#3: CGTAAATTTGCCAGAACTG); *Prkaa1* (sgRNA#1: CCTGTGACAATAATCCACAC; sgRNA#2: TGAAGGGTTAAGTACTGAG; sgRNA#3: GAAGATTCGGAGCCTTGACG); *Rosa26* (sgRNA#1: TGCAAGTTGAGTCCATCCGC; sgRNA#2: GGGTAAACGACTCCCCCAG); non-targeting control (GGAGCGCACCATCTTCTTCA).

*Human cells.* MOLM14 and OCI-AML2 cell lines were transduced with lentiviruses containing sgRNA targeting *PRKAA1* or a non-targeting sequence.<sup>14,15</sup> For AMPK add-back we transduced MOLM14 AMPK KO cells with a pLenti6-AMPK alpha1 1-312 that is not targeted by the *PRKAA1* sgRNA (Addgene plasmid #162131).<sup>16</sup>

### Lentiviral and retroviral infection

Virus was produced following standard methods in 293T cells using Lipofectamine 2000 (ThermoFisher #11668019) and either psPAX2 (2nd generation lentiviral packaging plasmid,



Addgene #12260) and pMD2.G (VSV-G envelope expressing plasmid, Addgene #12259) for lentivirus, or pECO-PAC2 for retrovirus.

### **MLL-AF9 mouse primary cell line generation**

All animal experiments were performed with approval from the DFCI IACUC. Murine ckit+ cells were sorted from whole bone marrow from Rosa26-Cas9 knock-in C57BL/6J mice, transduced with MLL-AF9 retrovirus and reinjected to sublethally irradiated C57BL/6J mice to generate a murine model of AML.<sup>17</sup> Mice were monitored by peripheral blood sampling and euthanized when overt AML was diagnosed (more than 20% circulating GFP positive blasts or poor body condition). Briefly, single cell suspensions from femurs and tibias of a leukemic mouse were harvested by spin-isolation<sup>18</sup> and seeded in methylcellulose media (Methocult, Stem Cell Technologies, M3234), supplemented with IL-6 (10 ng/ml), SCF (10 ng/ml), and IL-3 (6 ng/ml) (GoldBio). After serial replatings, when more than 90% of the colonies were CFU-G, cells were switched to liquid culture in media containing IL-3 (10 ng/ml, then 1 ng/ml). Cells were replated repeatedly and the %GFP positive were regularly monitored until the AML cells were able to grow in cytokine-free media (**Fig. 1D**). Dead cells were removed by magnetic separation following the manufacturer's instructions periodically (Dead Cell Removal kit, Miltenyi Biotec, 130-090-101).

### **Murine bone marrow-derived dendritic cells**

BMDCs were generated from bone marrow isolated from 8-10 week-old C57BL/6J mice.<sup>19</sup> Cells were isolated from leg bones by centrifugation<sup>18</sup>, then cultured in presence of recombinant murine granulocyte-macrophage colony stimulating factor (rmGM-CSF; 20 ng/mL) for 7 days. Fresh culture medium supplemented with rmGM-CSF was added at day 3. At day 7, the percent CD11c<sup>+</sup> cells (BMDCs) was determined by flow cytometry and used for further experiments.

### **Coculture experiments**

At day 6 of BMDC differentiation, murine AML cells (C1498 or MLL-AF9 transformed cells) were treated with drugs or vehicle in a separate flask. At day 7 of differentiation, BMDCs and tumor cells were mixed at a ratio ranging from 1:2 to 1:20. After overnight coculture, BMDC activation was measured by flow cytometry using CD11c (marker of DCs), with CD80, CD86, and MHCII (activation markers). As a positive control to induce activation markers without AML co-culture, BMDCs were incubated with 0.1 µg/ml lipopolysaccharide (LPS) overnight.

## **Vaccination assay**

6-8-week-old female C57BL/6J mice were obtained from The Jackson Laboratory. AML cells were treated in vitro for 24 h with GSK621 30  $\mu$ M or vehicle. After 24 h, the cells were fixed in formalin 1% (in PBS) and then washed 5 times in PBS, as described.<sup>20</sup> After the last wash, cells were resuspended in PBS at  $20 \times 10^6$  cells/ml. Mice received a first subcutaneous injection of 100  $\mu$ L ( $2 \times 10^6$  fixed cells) in the left flank, followed by an identical boost one week later in the same flank. One week after the vaccination boost, the animals were challenged with 850K live cells resuspended in 50% PBS:50% Matrigel, in the right flank. The group designated as unvaccinated received 100  $\mu$ L of PBS only for the two vaccination steps. All subcutaneous injections were done under isoflurane anesthesia. For T-cell depletion, animals received intraperitoneal injections of 200  $\mu$ g each of mouse anti-CD4 and anti-CD8 antibodies (InVivoMAb anti-mouse CD4, Clone: GK1.5, BioXcell #BE0003-1; InVivoMAb anti-mouse CD8 $\alpha$ , Clone 2.43, BioXcell # BE0061), or IgG control antibody (InVivoMAb rat IgG2b isotype control, BioXcell #BE0090). Injections of antibodies started 2 days prior to challenge and were continued until the end of the experiment. Tumor growth was monitored with digital calipers every 2-3 days. Tumor volumes were approximated by:  $\text{Volume} = (\text{Width}^2 \times \text{Length})/2$ , where Length is the longer tumor diameter and Width is the perpendicular tumor diameter. All experiments followed Institutional Animal Care and Use Committee approved protocols. The study endpoints were defined per animal facility policies and required euthanasia for any mouse bearing a subcutaneous tumor reaching 2 cm in any dimension, an ulcerated tumor, or overall poor body condition or distress.

## **Western blotting**

Cells were lysed in Laemmli buffer supplemented with DTT (50 mM) and sodium orthovanadate (2 mM). Blots were imaged using an Image Quant LAS-4000. Antibodies used were: Actin, MilliporeSigma #A5441; AMPK $\alpha$ , Cell Signaling Technology #2532S; ATF4, Cell Signaling Technology #11815S; Calreticulin, Cell Signaling Technology #12238S; Cas9, Cell Signaling Technology #14697S; CHOP, Cell Signaling Technology #2895S; eIF2 $\alpha$ , Cell Signaling Technology #9722S; ULK1, Cell Signaling Technology #8054S; Phospho-AMPK $\alpha$  (Thr172), Cell Signaling Technology #2535S; Phospho eIF2 $\alpha$  (Ser51), Cell Signaling Technology #3398S; Phospho-ULK1 (Ser555), Cell Signaling Technology #5869S.

## **Flow cytometry**

*Antibody staining.* Cells were washed in PBS (PBS 1X, pH 7.4; Gibco, 10010049) supplemented with 1% Bovine Serum Albumin (Fisher BioReagents, BP1600100) and incubated with Fc block, following the manufacturer's protocols (mouse: Anti-Mouse CD16-CD32, Thermo Fisher Scientific #BDB553141; Human BD Fc Block, # 564219). Cells were stained with indicated antibodies for 30 minutes at 4°C in the dark. *Apoptosis.* Cells were washed in binding buffer 1X (Annexin V Binding Buffer, Fisher Scientific, BDB556454) and incubated for 15 minutes at room temperature in the dark with fluorochrome conjugated Annexin V and live/dead dye. Cells were analyzed using a CytoFLEX S (Beckman Coulter) or a BD LSRFortessa™ X-20. At least 10,000 events in the population of interest were recorded. Data were analyzed using FlowJo v10.8 (BD Life Sciences). Reagents used: Propidium Iodide staining solution, Fisher Scientific #BDB556463; DAPI, Cell Signaling Technology #4083S; Zombie Green, BioLegend # 423111; Zombie Aqua, BioLegend #423101; Anti-Calreticulin antibody - ER Marker, Abcam #ab 2907; Goat anti-Rabbit IgG (H+L) Secondary Antibody, Alexa Fluor 488, Invitrogen # A-11034; Alexa Fluor 647 Anti-Calreticulin antibody [EPR3924] - ER Marker, Abcam # ab196159; APC anti-human CD45, BioLegend #368512; AnnexinV-Pacific Blue, BioLegend #640918; APC anti-mouse CD11c, BioLegend #117310; Brilliant Violet 510 anti-mouse CD86, BioLegend #105039; PE anti-mouse I-A/I-E (MHCII), BioLegend #107607; PerCP/Cyanine5.5 anti-mouse CD80, BioLegend #104721.

### **Statistical analyses**

Statistical analyses were performed using GraphPad Prism v9, GraphPad Software, La Jolla California USA. Statistical tests used for each data presentation are specified in the legends.

## Results

### GSK621 induces pre-apoptotic CALR membrane exposure in murine and human AML cells

We recently showed that AMPK activation by GSK621 induced a stress response through PERK activation and eIF2 $\alpha$  phosphorylation.<sup>12</sup> Given that eIF2 $\alpha$  phosphorylation is a hallmark of ICD, we hypothesized that GSK621 might elicit CALR membrane exposure and enhanced adjuvanticity in AML. We first tested the effects of GSK621 on the C1498 murine AML cell line<sup>21</sup>, derived from a spontaneous leukemia in a C57BL/6 mouse (**Fig. S1A**). GSK621 induced dose-dependent apoptosis after 48 h of exposure, similar to the effects seen in human AML cells<sup>14</sup> (**Fig. 1A**). Next, to establish controls for the specificity of surface CALR quantification by flow cytometry, we generated positive control C1498 cells with constitutive CALR membrane expression, or negative control cells with *Calr* knockout (KO) using CRISPR-Cas9 (**Fig. S1B**). We observed that CALR staining was similar to isotype control in *Calr* KO cells, while signal intensity was markedly increased in cells with enforced CALR surface expression (**Fig. 1B and S1C**). We next treated parental C1498 cells with GSK621 and observed that CALR membrane expression increased within 6 hours in a dose-dependent manner (**Fig. 1C and S1D**), supporting the hypothesis that AMPK activation induces ICD. CALR expression was also induced by mitoxantrone (MTO), an anthracycline known to induce ICD.<sup>22</sup> In contrast, the antileukemic drug cytarabine (AraC) did not induce CALR membrane expression to the same level (**Fig. 1C**), despite inducing a comparable degree of cell death (**Fig. S1E**).

To test this hypothesis in a distinct and genetically defined AML model, we transduced bone marrow cells from C57BL/6 mice to express the human MLL-AF9 (also known as *KMT2A::MLLT3*) fusion oncogene. Subsequent transplantation into syngeneic recipient mice led to leukemia development, as performed previously.<sup>23</sup> We cultured the resulting mouse AML cells ex vivo in methylcellulose and performed serial replating to generate a murine AML cell

line (designated MLL-AF9 cells) (**Fig. 1D**). In these AML cells, GSK621 treatment for 48 h induced dose-dependent apoptosis (**Fig. 1E**), which was preceded by CALR surface exposure in viable cells at 24 h of drug exposure (**Fig. 1F-G**).

Finally, we exposed bone marrow samples from three patients with AML (**Suppl. Table 1**) to GSK621. We observed increased CALR membrane expression in live bone marrow blasts at levels comparable to those induced by MTO (**Fig. 1H-I**). Interestingly, induction of apoptosis and CALR exposure were detected on leukemia blasts but not on granulocytes and lymphocytes from the same bone marrow sample, which supports a potential therapeutic window (**Fig. S1F**). Collectively, these results show that GSK621 induces an immunostimulatory DAMP in the form of CALR membrane exposure in murine and human leukemia cells.

### **Calreticulin surface exposure is dependent on AMPK**

To determine if CALR membrane exposure induced by GSK621 was AMPK dependent, we used MOLM-14 and OCI-AML2 human AML cell lines depleted of the AMPK $\alpha$ 1 subunit by CRISPR-Cas9 editing (AMPK KO), which fully abrogates AMPK activity<sup>14</sup> (**Fig. 2A**). We observed that incubation with GSK621 had no impact on whole cell CALR protein abundance in AMPK KO or in control (non-targeted sgRNA, NTG) cells (**Fig. S2A**). However, CALR cell surface expression was strongly induced by GSK621 in control but not in AMPK KO cells, arguing that GSK621-induced CALR membrane upregulation was on-target (**Fig. 2B-C**). GSK621 did not possess intrinsic fluorescence or promote isotype control staining, further supporting the specificity of cell surface CALR detection (**Fig. S2C**). In contrast, CALR membrane exposure was strongly increased by idarubicin, an anti-AML chemotherapy known to induce ICD<sup>22</sup>, in cells with or without AMPK (**Fig. 2D**). Other anti-AML chemotherapies, such as cytarabine and venetoclax, had less impact on CALR membrane exposure (**Fig. 2D**). Notably,

all these agents caused comparable cell death in MOLM-14 cells at the same concentrations, supporting that specific cytotoxic drugs induce CALR exposure (**Fig S2B**).

To confirm target specificity, in AMPK KO cells we re-expressed an active truncated form of AMPK (AMPK 1-312, missing an inhibitory domain<sup>16</sup>) that is not targeted by the AMPK sgRNA (**Fig. 2E-F, Fig. S2D**). Expression of AMPK 1-312 allowed membrane CALR induction in AMPK KO cells treated with GSK621 (**Fig. 2F**). This was in contrast to treatment with venetoclax or cytarabine, which did not induce surface CALR regardless of AMPK expression status (**Fig. 2F**). These data support a model in which CALR exposure can be induced in AML by specific agents and via AMPK-dependent or AMPK-independent pathways.

We recently showed that AMPK activation by GSK621 induces an ER stress response dependent on PERK activation.<sup>12</sup> As the integrated stress response is known to induce CALR membrane exposure and ICD<sup>9,24</sup>, we investigated the role of PERK in AMPK-induced CALR membrane expression. We used PERK knockout MOLM-14 cells in which we could conditionally re-express PERK by a doxycycline-inducible construct.<sup>12</sup> We observed that PERK expression was important for eIF2 $\alpha$  phosphorylation induced by GSK621 (**Fig. 2G**). Moreover, CALR membrane expression was enhanced by GSK621 treatment in PERK-expressing MOLM-14 cells but was unaffected by PERK expression in the absence of GSK621 (**Fig. 2H**). Collectively, these results show that AMPK activation by GSK621 induced ICD markers, including eIF2 $\alpha$  phosphorylation and CALR membrane exposure, which were at least partially dependent on PERK.

### **AML cells pretreated with GSK621 induce bone marrow dendritic cell maturation**

Maturation of antigen presenting cells is a surrogate readout of tumor cell immunogenicity in co-culture experiments.<sup>25</sup> We examined the effect of GSK621-treated murine AML cells on

syngeneic bone marrow-derived DCs (BMDCs) in coculture assays *ex vivo*. We used lipopolysaccharide (LPS) as a positive control to induce direct BMDC activation and maturation.<sup>26</sup> We first incubated C1498 cells with vehicle (DMSO), GSK621, MTO, or AraC. These cells were then co-cultured with syngeneic BMDCs, and we measured DC activation by the expression of CD80 or CD86 among CD11c and MHCII positive BMDCs, using two ratios of DCs to tumor cells to mimic the heterogeneity of bone marrow infiltration in patients with AML (**Fig. 3A, Fig. S3A**). We observed that C1498 cells previously exposed to GSK621 or MTO significantly induced CD80 and CD86 expression on BMDCs to a level similar to LPS-treated BMDCs, while AraC-treated cells induced more modest BMDC maturation (**Fig. 3B-C**). As an additional control, we used 3 cycles of freeze/thaw to induce nonspecific death in AML cells. We observed that a 1:1 or 1:10 ratio of DCs to freeze/thaw-killed tumor cells was insufficient to trigger BMDC activation (**Fig. S3B-C**). We repeated this assay using GSK621-treated MLL-AF9 AML cells and similarly observed that co-culture with BMDCs significantly induced CD80<sup>+</sup> and CD86<sup>+</sup> expression (**Fig. 3D**). Together, these results show that AMPK activation in AML cells enables them to induce DC maturation.

### **GSK621 treated AMLs induce a vaccination effect *in vivo* in immunocompetent mice**

To establish that AMPK activation results in clinically-relevant ICD, we investigated the potential of GSK621-treated cells to facilitate an anti-tumor immune response *in vivo* using vaccination assays.<sup>25</sup> In these experiments, syngeneic murine AML cells were incubated *in vitro* with GSK621, and then injected subcutaneously into the left flank of immunocompetent C57BL/6 mice (vaccine site). After seven days, we injected live AML cells into the right flank of vaccinated mice (challenge site) and followed tumor growth on the challenge site (**Fig. 4A**). In the first experiment using C1498 AML cells, we observed that mice vaccinated with GSK621 or AraC treated cells had significantly reduced tumor growth and improved tumor-free survival compared to unvaccinated mice (**Fig. S4A-B**). However, there was no statistical difference

between the GSK621 and AraC groups, possibly due to the rapid growth of C1498 cells in all assay arms using this model. Indeed, all animals vaccinated with DMSO-treated cells had to be censored because they developed tumors at the vaccination site before the challenge site could be assessed. Nonetheless, using an ELISpot assay we confirmed that splenocytes from mice vaccinated with GSK621-treated AML produced IFN $\gamma$  when cultured specifically in the presence of parental leukemia cells (**Fig. 4B**), which suggested the induction of tumor-specific cellular immunity.

To overcome the problem of aggressive growth of the untreated vaccine cells, we performed similar experiments using MLL-AF9-driven AMLs and modified our protocol by fixing treated cells before vaccination using 1% formalin, which is known to preserve the expression of cell surface molecules for tumor immunization.<sup>20</sup> We observed that the difference in CALR staining between GSK621 and vehicle-treated cells after fixation (**Fig. S4C**) was similar to that seen in unfixed cells. Using this model, we observed an absence of tumor growth at the challenge site and 100% survival in the cohort of mice vaccinated with GSK621-treated AML cells, which was statistically improved compared with the other groups (**Fig. 4C-D**). To explore the role of cellular immunity in the vaccination effect, we performed the same experiment in recipient mice treated with antibodies to deplete T-cells prior to challenge. We reproduced the vaccination effect induced by GSK621-treated cells in immunocompetent mice receiving control IgG antibodies. In contrast, all CD4/CD8-depleted mice developed tumors that led to 100% mortality of this cohort, showing that the protective antitumor immune response induced by AMPK-activated leukemic cells was dependent on T cells in the vaccine recipients (**Fig. 4E-F**). Collectively, these results indicate that AMPK activation by GSK621 elicits immunogenic cell death in AML models.

## Discussion



AML has been treated by alloHSCT for decades, a modality of immunotherapy in which graft-versus-leukemia activity is achieved by T-cells and NK-cells from the donor.<sup>27</sup> However, the anti-leukemic activity of alloHSCT is for the most part inseparable from graft-versus-host disease, which causes considerable morbidity and mortality.<sup>28</sup> Therefore, improving cellular immunity to eradicate leukemic cells represents an important therapeutic goal. Directing T-cells toward leukemia cells may be achieved by T-cell recruiting antibody constructs such as bispecific T-cell engagers (BiTEs) against leukemia antigens, or by immune checkpoint inhibitors such as anti-PD-1/PD-L1 antibodies.<sup>4</sup> Moreover, autologous T-cells can be modified to express chimeric antigen receptors targeting AML antigens such as CD33 and CD123.<sup>29</sup> However, while bone marrow infiltrating T-cell number is preserved or even increased in patients with AML compared to healthy individuals, they are functionally impaired.<sup>30</sup> This impairment may drive the disappointing results of T-cell immunotherapies to date. Immune evasion may involve defective antigen presentation, upregulation of checkpoint molecules, and other mechanisms of direct suppression of immune cells.<sup>31</sup> Therefore, new strategies enhancing leukemia adjuvanticity could represent an improvement for AML immunotherapy.<sup>32</sup>

Here, we showed that AMPK activation using the small molecule GSK621 resulted in the expression of an immunostimulatory DAMP in the form of CALR membrane exposure by murine and human AML cells. We previously demonstrated that AMPK activation induced a stress response involving the PERK/eIF2 $\alpha$ /ATF4 signaling pathway resulting in mitochondrial priming.<sup>12</sup> Interestingly, here we found that CALR membrane exposure induced by GSK621 in pre-apoptotic leukemic cells was dependent on AMPK and involved eIF2 $\alpha$  phosphorylation. However, AMPK-induced CALR membrane expression was only partly dependent on PERK, suggesting that other effectors downstream of AMPK contributed to this immunostimulatory signal in AML. In melanoma, the stress kinases PKR and GCN2 were shown to be key mediators of eIF2 $\alpha$  phosphorylation *in vitro*<sup>33</sup> and might be pathways to explore in future work.

CALR surface exposure is associated with increased circulating NK, CD4<sup>+</sup>, and CD8<sup>+</sup> cell populations including T-cells directed against leukemia-associated antigens, and correlates with improved survival in patients with AML.<sup>34</sup> This suggests that pharmacological activation of AMPK to increase CALR could represent a new strategy to increase the anti-cancer immune response. We observed that idarubicin, a widely used anti-AML chemotherapy, also strongly induced CALR membrane exposure in AML, as reported<sup>35</sup>, and was independent of AMPK. However, previous work demonstrated that PERK was necessary for anthracycline-induced surface calreticulin exposure<sup>36</sup>, which suggests a possible crosstalk between the DNA damage response and ER stress, independent of AMPK.<sup>37</sup> The precise mechanism of other anti-leukemic therapies' induction of ICD should be studied in future experiments.

This prompts the question of why not simply rely on conventional chemotherapy to induce ICD in AML? In addition to causing myelosuppression and organ toxicity, anthracyclines have immunosuppressive activity by increasing regulatory T-cells (Tregs) and tolerogenic DCs, which may limit anti-leukemia immunity.<sup>38</sup> Cytarabine is reported to modulate checkpoint molecules and possibly promote AML immunogenicity.<sup>39</sup> However, we observed that cytarabine did not induce CALR membrane exposure to the same degree as GSK621, and it only modestly primed leukemic cells to trigger BMDC maturation *ex vivo*. Thus, the "3+7" induction regimen of anthracycline plus cytarabine that is the backbone of AML therapy has complex effects on immunity, which might still be enhanced by adding AMPK agonism. In further support of using AMPK activation as immune stimulation, AMPK loss in Tregs promotes tumor growth by increasing the expression of PD-1, while treatment of Tregs with the AMPK activator AICAR decreases PD-1 expression.<sup>40</sup> This suggests that AMPK activation could exert anti-cancer immunostimulatory effects on the tumor microenvironment as well as on AML cells. In fact, trials have reported activity combining immune checkpoint blockade with metformin, an inhibitor of complex I mitochondria respiratory chain that stimulates anti-cancer immunity in part through

AMPK activation.<sup>41</sup> Together, our results suggest that AMPK activation could represent an attractive strategy to kill AML blasts and simultaneously increase their adjuvanticity. Alternatively, addition of AMPK activation to conventional AML chemotherapies might enhance immunogenicity without relying solely on the AMPK activator for tumor debulking.

To establish that AMPK activation resulted in ICD, we used vaccination assays in AML models in syngeneic immunocompetent mice. Even though AML mainly spreads in bone marrow and blood, we challenged vaccinated mice by the subcutaneous injection of leukemic cells, leading to the development of in situ tumors using established tumor immunology assays.<sup>14</sup> This provided straightforward and reproducible measurements of tumor growth. In future studies, it may be important to test systemic leukemia growth, as AML cells may interact differently with the immune system in bone marrow, blood, and in lymphoid organs such as spleen. Despite these limitations, pre-treatment of either C1498 or MLL-AF9 driven AML cells by GSK621 was able to induce a robust vaccination effect in vivo that was dependent on a T-cell systemic adaptive immune response specific to AML blasts.

In summary, we show that DAMP production by GSK621-treated AML cells primes BMDCs in vitro and elicits an adaptive T-cell immune response in vivo in immunocompetent hosts. This strategy could be exploited to increase AML adjuvanticity to improve endogenous immune responses and/or the efficacy of T-cell based immunotherapies. The best timing of such treatments should be determined in clinical trials, possibly as an “immune priming” before or during initiation of induction chemotherapy, or later as part of consolidation. For instance, AMPK activation could be combined with other immunotherapies for patients who have achieved chemotherapy-induced remission, such as with dendritic cell-AML fusion vaccines<sup>42</sup> or immune checkpoint blockade.



## Acknowledgements

The authors thank the Translational Immunogenomics Lab at the Dana-Farber Cancer Institute, in particular Derin Keskin, for scientific advice and technical support for immune monitoring ex vivo. The authors thank Sabrina Spaggiari from Institut Gustave Roussy for technical support and advice in preliminary in vitro experiments.

## Authorship Contributions

JM: conceptualization, resources, data curation, data analysis, supervision, funding acquisition, validation, investigation, methodology, writing—original draft; MG, LP: resources, data analysis, investigation, methodology; RAB: investigation; OK, GK: methodology; JES: resources, methodology; JT, AAL: conceptualization, resources, supervision, funding acquisition, writing—review and editing.

## Funding and Disclosures of Conflicts of Interest

JM was funded by the French National Institute for Health and Medical Research (INSERM, *Plan Cancer InCa - formation à la recherche translationnelle en cancerologie*), the French Ligue Against Cancer, The Monahan Foundation (partner of the Fullbright Foundation), and L'Oréal-UNESCO for Women in Science French Young Talents program. MG was funded by the Cancéropôle Grand Sud-Ouest (GSO). MG, LP, and JES report funding from the Laboratoire d'Excellence Toulouse Cancer (TOUCAN and TOUCAN2.0; contract ANR11-LABEX), INCA (PLBIO 2020-010, DIALAML), the Fondation ARC, and the Ligue National de Lutte Contre le Cancer. OK reports grants from the French Institut National du Cancer (INCA) and the DIM Elicit initiative of the Ile de France. This work was supported by grants from the French Institut National du Cancer (INCA) through the *Site de Recherche Intégrée sur le Cancer* (SIRIC) Cancer Research for Personalized Medicine (CARPEM). AAL was funded by the National Institutes of Health/National Cancer Institute CA225191, the Ludwig Center at Harvard, Alex's Lemonade Stand Foundation, and is a Scholar of the Leukemia & Lymphoma Society. OK is a cofounder of Samsara Therapeutics. GK declares having held research contracts with Daiichi Sankyo, Eleor, Kaleido, Lytix Pharma, PharmaMar, Osasuna Therapeutics, Samsara Therapeutics, Sanofi, Sotio, Tollys, Vascage and Vasculox/Tioma, has received consulting/advisory honoraria from Reithera, is on the Board of Directors of the Bristol Myers Squibb Foundation France, is a scientific co-founder of everImmune, Osasuna Therapeutics, Samsara Therapeutics and Therafast Bio, and is the inventor of patents covering therapeutic targeting of aging, cancer, cystic fibrosis and metabolic disorders. AAL has received research funding from AbbVie and Stemline Therapeutics, and consulting fees from Adaptimmune, Cimeio, IDRx, N-of-one, Qiagen, and Stemline Therapeutics.

## References

1. DiNardo CD, Wei AH. How I treat acute myeloid leukemia in the era of new drugs. *Blood*. 2020;135(2):85–96.
2. Bokhari SW, Watson L, Nagra S, et al. Role of HCT-comorbidity index, age and disease status at transplantation in predicting survival and non-relapse mortality in patients with myelodysplasia and leukemia undergoing reduced-intensity-conditioning hemopoietic progenitor cell transplantation. *Bone Marrow Transplant*. 2012;47(4):528–534.
3. Carré M, Porcher R, Finke J, et al. Role of Age and Hematopoietic Cell Transplantation-Specific Comorbidity Index in Myelodysplastic Patients Undergoing an Allograft: A Retrospective Study from the Chronic Malignancies Working Party of the European Group for Blood and Marrow Transplantation. *Biol. Blood Marrow Transplant. J. Am. Soc. Blood Marrow Transplant*. 2020;26(3):451–457.
4. Daver N, Alotaibi AS, Bücklein V, Subklewe M. T-cell-based immunotherapy of acute myeloid leukemia: current concepts and future developments. *Leukemia*. 2021;35(7):1843–1863.
5. Vago L, Gojo I. Immune escape and immunotherapy of acute myeloid leukemia. *J. Clin. Invest*. 2020;130(4):1552–1564.
6. Galluzzi L, Vitale I, Aaronson SA, et al. Molecular mechanisms of cell death: recommendations of the Nomenclature Committee on Cell Death 2018. *Cell Death Differ*. 2018;25(3):486–541.
7. Jang G-Y, Lee J won, Kim YS, et al. Interactions between tumor-derived proteins and Toll-like receptors. *Exp. Mol. Med*. 2020;52(12):1926–1935.
8. Kroemer G, Galassi C, Zitvogel L, Galluzzi L. Immunogenic cell stress and death. *Nat. Immunol*. 2022;23(4):487–500.
9. Bezu L. eIF2alpha phosphorylation is pathognomonic for immunogenic cell death. *Cell Death Differ*. 2018;25:1375–1393.
10. Hetz C, Zhang K, Kaufman RJ. Mechanisms, regulation and functions of the unfolded protein response. *Nat. Rev. Mol. Cell Biol*. 2020;21(8):421–438.
11. Fucikova J, Spisek R, Kroemer G, Galluzzi L. Calreticulin and cancer. *Cell Res*. 2021;31(1):5–16.
12. Grenier A, Poulain L, Mondesir J, et al. AMPK-PERK axis represses oxidative metabolism and enhances apoptotic priming of mitochondria in acute myeloid leukemia. *Cell Rep*. 2022;38(1):.
13. Chen X, Fosco D, Kline DE, Kline J. Calreticulin promotes immunity and type I interferon-dependent survival in mice with acute myeloid leukemia. *Oncoimmunology*. 2017;6(4):e1278332.
14. Sujobert P, Poulain L, Paubelle E, et al. Co-activation of AMPK and mTORC1 Induces Cytotoxicity in Acute Myeloid Leukemia. *Cell Rep*. 2015;11(9):1446–1457.
15. Grenier A, Sujobert P, Olivier S, et al. Knockdown of Human AMPK Using the CRISPR/Cas9 Genome-Editing System. *Methods Mol. Biol. Clifton NJ*. 2018;1732:171–194.
16. Liu X, Xiao Z-D, Han L, et al. LncRNA NBR2 engages a metabolic checkpoint by regulating AMPK under energy stress. *Nat. Cell Biol*. 2016;18(4):431–442.
17. Chen W, Kumar AR, Hudson WA, et al. Malignant Transformation Initiated by MII-AF9: Gene Dosage and Critical Target Cells. *Cancer Cell*. 2008;13(5):432–440.
18. Heib T, Gross C, Müller M-L, Stegner D, Pleines I. Isolation of murine bone marrow by centrifugation or flushing for the analysis of hematopoietic cells - a comparative study. *Platelets*. 2021;32(5):601–607.
19. Madaan A, Verma R, Singh AT, Jain SK, Jaggi M. A stepwise procedure for isolation of murine bone marrow and generation of dendritic cells. *J. Biol. Methods*. 2014;1(1):1.

20. Obata C, Zhang M, Moroi Y, et al. Formalin-fixed tumor cells effectively induce antitumor immunity both in prophylactic and therapeutic conditions. *J. Dermatol. Sci.* 2004;34(3):209–219.
21. Mopin A, Driss V, Brinster C. A Detailed Protocol for Characterizing the Murine C1498 Cell Line and its Associated Leukemia Mouse Model. *J. Vis. Exp.* 2016;(116):.
22. Fucikova J, Kepp O, Kasikova L, et al. Detection of immunogenic cell death and its relevance for cancer therapy. *Cell Death Dis.* 2020;11(11):1013.
23. Somerville TCP, Cleary ML. Identification and characterization of leukemia stem cells in murine MLL-AF9 acute myeloid leukemia. *Cancer Cell.* 2006;10(4):257–268.
24. Panaretakis T. Mechanisms of pre-apoptotic calreticulin exposure in immunogenic cell death. *EMBO J.* 2009;28:578–590.
25. Galluzzi L. Consensus guidelines for the definition, detection and interpretation of immunogenic cell death. *J Immunother Cancer.* 2020;8:000337.
26. Poltorak A, Smirnova I, He X, et al. Genetic and physical mapping of the Lps locus: identification of the toll-4 receptor as a candidate gene in the critical region. *Blood Cells. Mol. Dis.* 1998;24(3):340–355.
27. Powles R. 50 years of allogeneic bone-marrow transplantation. *Lancet Oncol.* 2010;11(4):305–306.
28. Arai S, Arora M, Wang T, et al. Increasing incidence of chronic graft-versus-host disease in allogeneic transplantation: a report from the Center for International Blood and Marrow Transplant Research. *Biol. Blood Marrow Transplant. J. Am. Soc. Blood Marrow Transplant.* 2015;21(2):266–274.
29. Mardiana S, Gill S. CAR T Cells for Acute Myeloid Leukemia: State of the Art and Future Directions. *Front. Oncol.* 2020;10:697.
30. Lambie AJ, Kosaka Y, Laderas T, et al. Reversible suppression of T cell function in the bone marrow microenvironment of acute myeloid leukemia. *Proc. Natl. Acad. Sci.* 2020;117(25):14331–14341.
31. Tettamanti S, Pievani A, Biondi A, Dotti G, Serafini M. Catch me if you can: how AML and its niche escape immunotherapy. *Leukemia.* 2022;36(1):13–22.
32. Pfirschke C. Immunogenic chemotherapy sensitizes tumors to checkpoint blockade therapy. *Immunity.* 2016;44:343–354.
33. Giglio P. PKR and GCN2 stress kinases promote an ER stressindependent eIF2alpha phosphorylation responsible for calreticulin exposure in melanoma cells. *Oncoimmunology.* 2018;7:1466765.
34. Fucikova J. Calreticulin exposure by malignant blasts correlates with robust anticancer immunity and improved clinical outcome in AML patients. *Blood.* 2016;128:3113–3124.
35. Kroemer G, Galluzzi L, Kepp O. Immunogenic cell death in cancer therapy. *Annu Rev Immunol.* 2013;31:51–72.
36. Panaretakis T, Kepp O, Brockmeier U, et al. Mechanisms of pre-apoptotic calreticulin exposure in immunogenic cell death. *EMBO J.* 2009;28(5):578–590.
37. González-Quiroz M, Blondel A, Sagredo A, et al. When Endoplasmic Reticulum Proteostasis Meets the DNA Damage Response. *Trends Cell Biol.* 2020;30(11):881–891.
38. Lecciso M, Ocadlikova D, Sangaletti S, et al. ATP Release from Chemotherapy-Treated Dying Leukemia Cells Elicits an Immune Suppressive Effect by Increasing Regulatory T Cells and Tolerogenic Dendritic Cells. *Front. Immunol.* 2017;8:.
39. Pinto A, Maio M, Attadia V, Zappacosta S, Cimino R. Modulation of HLA-DR antigens expression in human myeloid leukaemia cells by cytarabine and 5-aza-2'-deoxycytidine. *Lancet Lond. Engl.* 1984;2(8407):867–868.
40. Pokhrel RH, Acharya S, Ahn J-H, et al. AMPK promotes antitumor immunity by downregulating PD-1 in regulatory T cells via the HMGR/p38 signaling pathway. *Mol. Cancer.* 2021;20(1):133.

41. Liu W, Wang Y, Luo J, Liu M, Luo Z. Pleiotropic Effects of Metformin on the Antitumor Efficiency of Immune Checkpoint Inhibitors. *Front. Immunol.* 2021;11:3724.
42. Rosenblatt J, Stone RM, Uhl L, et al. Individualized vaccination of AML patients in remission is associated with induction of antileukemia immunity and prolonged remissions. *Sci. Transl. Med.* 2016;8:368–171.



## Figure Legends

**Figure 1. GSK621 induces pre-apoptotic surface calreticulin exposure in murine and human cells.** (A) C1498 cells were treated at the indicated concentrations with GSK621 for 48 hours and percentage apoptotic cells was measured by flow cytometry using AnnexinV/propidium iodide (PI) staining (early apoptotic cells: AnnexinV+/PI-; late apoptotic: AnnexinV+/PI+). Ordinary two-way Anova with Dunnet's multiple comparisons test. (B) Flow cytometry of C1498 cells used as controls for surface calreticulin staining. CALR KO or constitutive cell surface CALR were stained with a calreticulin-AF647 antibody or isotype control. Graphs represent mean fluorescence intensity +/- SD. (C) Fold change in mean fluorescence intensity (MFI) relative to vehicle of surface calreticulin staining on live, unpermeabilized cells by flow cytometry (MFI+/-SEM) after 6 h of treatment with the indicated drugs (GSK621, MTO, or cytarabine, AraC); n=3 biological replicates. Ordinary two-way Anova with Dunnet's multiple comparisons test. (D) Schematic of the procedure to generate MLL-AF9 transformed AML cells from leukemia bearing mice. After multiple replatings in methylcellulose supplemented with IL-6 (10 ng/ml), SCF (10 ng/ml), and IL-3 (6 ng/ml), colonies were enriched in CFU-G (picture). Colonies were then transferred in liquid media and grown in suspension. (E) MLL-AF9 cells were treated at various concentrations with GSK621 for 48 hours and percentages of apoptotic cells were measured as above. Ordinary two-way Anova with Sidak's multiple comparisons test. (F) Representative dot plots of surface CALR staining in unpermeabilized MLL-AF9 cells treated for 24 hours with GSK621 30  $\mu$ M or DMSO. (G) MFI of surface CALR staining measured on live, unpermeabilized MLL-AF9 cells; n=3 replicates. Paired t-test. (H) Percent of CALR+ PI- blasts of 3 samples from patients with AML after treatment with GSK621 20  $\mu$ M, MTO 0.5 nM, or DMSO. Human AML samples #1 and #2 were cryopreserved, thawed, and treated with GSK621. Sample #3 was received fresh and treated immediately. Ordinary one-way Anova with Dunnet's multiple comparisons test. (I) Representative dot plots for sample #3.

**Figure 2. Calreticulin surface exposure is AMPK-dependent in AML cells.** (A) Western blot showing knock-down efficiency of AMPK $\alpha$  in MOLM14 and OCI-AML2 cells transduced with a non-targeting control sgRNA guide (NTG) or *PRKAA1* sgRNA. (B) Representative dot plots of MOLM14 and OCI-AML2 surface CALR. Percentages represent the fraction of CALR+ among DAPI negative cells. (C) Control (NTG) or AMPK KO MOLM14 and OCI-AML2 cells were treated with GSK621 30  $\mu$ M or vehicle for 24 h and surface exposure of CALR was measured by flow cytometry. Results are MFI of CALR on live (DAPI negative) cells. Baseline fluorescence intensity of the isotype control stained or unstained DMSO treated cells are shown on the same graphs. Ordinary one-way Anova with Sidak's multiple comparisons test. (D) MOLM14 AMPK KO or control cells (MOLM14 NTG) were treated for 24 h with DMSO, GSK621 30  $\mu$ M, idarubicin (IDA) 25 nM, venetoclax (VEN) 500 nM, or cytarabine (AraC) 2  $\mu$ M and surface CALR was measured by flow cytometry. The MFI of three independent replicates is shown. Ordinary two-way Anova with Dunnet's multiple comparisons test for comparison to DMSO within each cell line group (NTG and AMPK KO), and Ordinary two-way Anova with Tukey's multiple comparisons test to compare GSK621 treatment in the NTG versus AMPK KO cell line. (E)

Western blot showing the expression of a V5-tagged truncated form of AMPK $\alpha$ 1 lacking its regulatory region (AMPK 1-312; selected in blasticidin; predicted size: 40kDa). (F) MFI of surface CALR on AMPK KO MOLM14 cells with or without AMPK (1-312) rescue after 24 h treatment with DMSO, GSK621, VEN, or AraC. Ordinary two-way Anova with Sidak's multiple comparisons test. (G) MOLM14 cells lacking endogenous PERK expression were generated by CRISPR-Cas9 editing of *EIF2AK3* at an intron-exon junction, compared to NTG cells. Cells were rescued with doxycycline-inducible expression of WT PERK bearing a Myc 9E10 tag. Western blot showing the indicated proteins in PERK knockdown and rescue cells with and without treatment with GSK621 30  $\mu$ M. (H) Surface exposure of CALR was measured by flow cytometry before and after induction of PERK rescue, with or without GSK621 treatment. Ordinary two-way Anova with Sidak's multiple comparisons test.

**Figure 3. AML cells pre-treated with GSK621 induce murine BMDC maturation in vitro.** (A) Experimental schema for coculture experiments. Bone marrow derived DCs (BMDCs) were generated over 7 days from fresh bone marrow cells harvested from female C57BL/6 mice. BMDC maturation was measured by flow cytometry after overnight coculture with tumor cells pretreated for 24 h prior to mixing. (B) Representative dot plots of the percent activated DCs after overnight coculture with cells pretreated with DMSO, AraC 10  $\mu$ M, GSK621 30  $\mu$ M, or MTO 100 nM, with a 1 DC:2 tumor cell ratio. Controls are BMDCs treated overnight with LPS 0.1  $\mu$ g/ml or vehicle (PBS). (C) Graphs representing the level of maturation of BMDCs as measured by percentage of MHCII<sup>+</sup>CD80<sup>+</sup> or MHCII<sup>+</sup>CD86<sup>+</sup> cells after overnight coculture with C1498 cells pre-treated as indicated, with 2 ratios of BMDC to tumor cells; n=3 replicates (mean $\pm$ -SD). BMDCs alone were treated with LPS as a positive control to induce activation markers. Ordinary one-way Anova with Dunnet's multiple comparisons test for multiple comparison to DMSO within each ratio of cocultures, and a t test to compare BMDC cultured without tumor cells, with or without LPS. (D) Coculture experiments using murine AML cells driven by MLL-AF9. Cells were pre-treated for 24 h with GSK621 or vehicle then mixed overnight with BMDCs in a 1 to 8 ratio (1 BMDC for 8 AML cells). Percent of live coculture-matured DCs as defined by DAPI negative, CD11<sup>+</sup> cells expressing MHCII and CD80 or MHCII and CD86 measured by flow cytometry. Ordinary one-way Anova with Sidak's multiple comparisons test.

**Figure 4. AML cells pre-treated with GSK621 induce a vaccination effect in vivo.** (A) Schema of the vaccination assay performed with C1498 cells or MLL-AF9 cells in immunocompetent C57BL/6 mice. (B) Representative IFN $\gamma$  ELISpot assay using single cell suspensions from the spleens of one animal of each arm of the experiment activated by culture with the parental AML cells. Splenocytes were cocultured with a syngeneic C57BL/6 melanoma cell line (B16F10) or the ovalbumin antigen alone (OVA) as negative controls, or anti-CD3 as a non-specific positive control. Each column represents ELISpots from splenocytes of one spleen seeded in triplicates. (C) Kaplan-Meier curves showing the overall survival in each group (5 mice per group) vaccinated with MLL-AF9 cells pretreated as indicated and fixed prior to injection, then challenged with live MLL-AF9 cells. Log Rank test. (D) Tumor growth on the challenge site of individual animals in panel (C). Of note, none of the mice vaccinated with

GSK621-treated cells developed tumors (red line on x-axis). (E) Kaplan-Meier curves showing the overall survival in each group (5 mice per group) vaccinated with MLL-AF9 cells pretreated with GSK621 prior to injection, then challenged with live MLL-AF9 cells. One group was depleted of CD4/CD8 T cells with intraperitoneal injections of neutralizing antibodies starting 2 days prior to the challenge (dashed line). The mice of the other group received a control IgG (solid line). Log Rank test. (F) Tumor growth on the challenge site of individual animals in panel (E).

# Figure 1

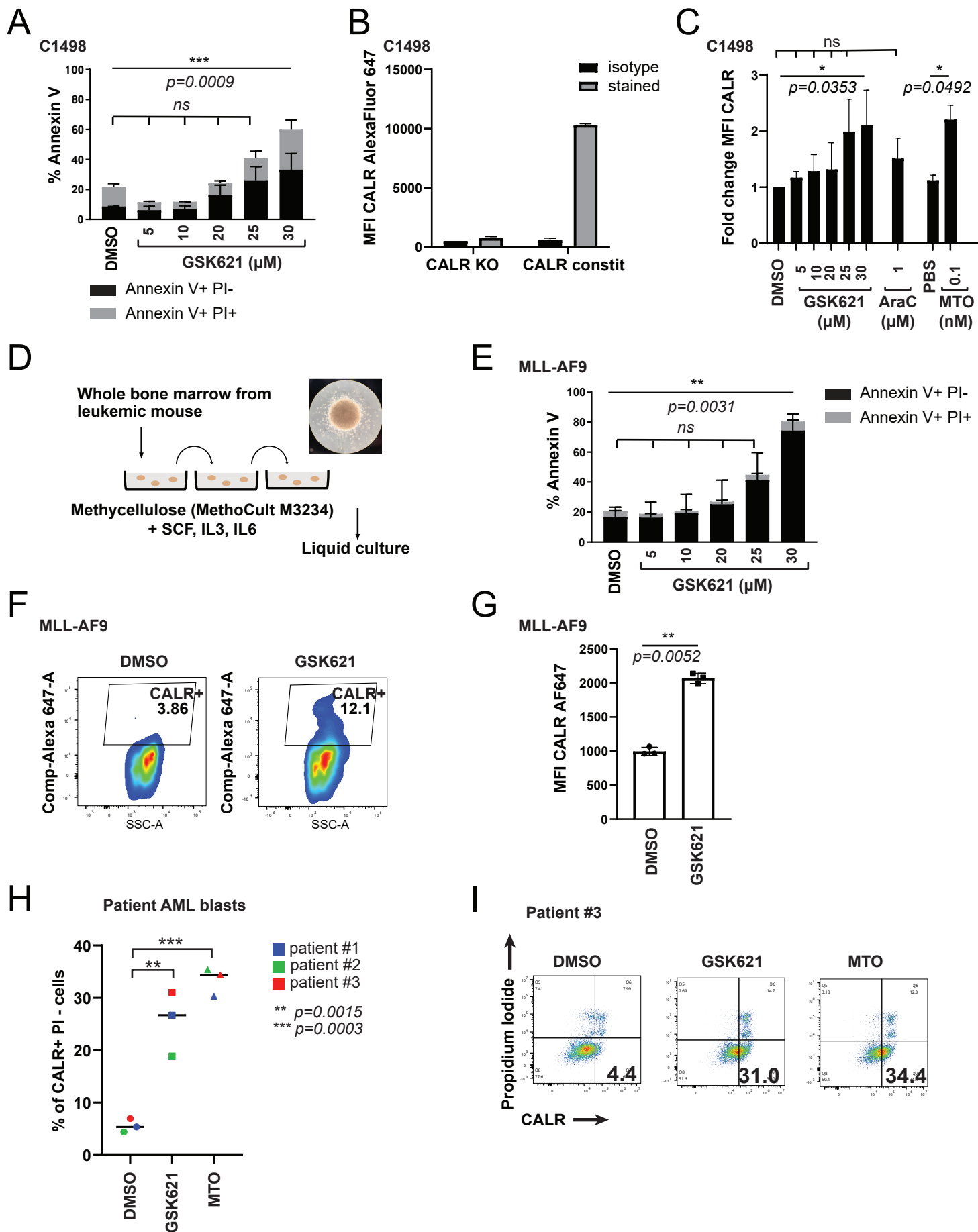
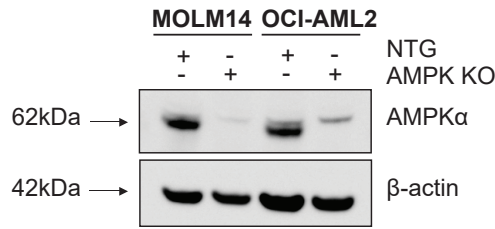
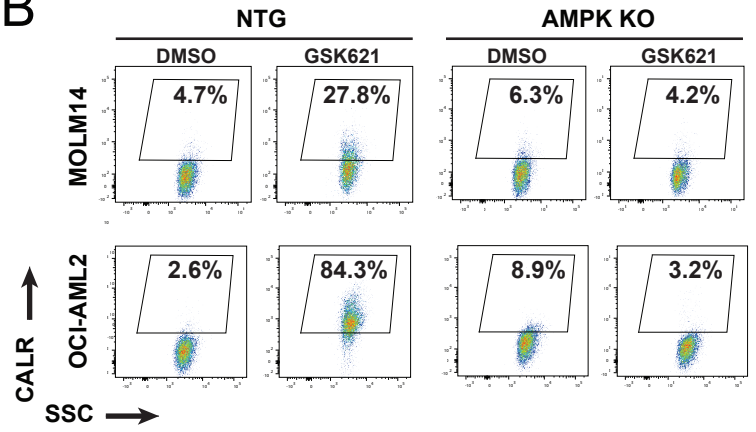


Figure 2

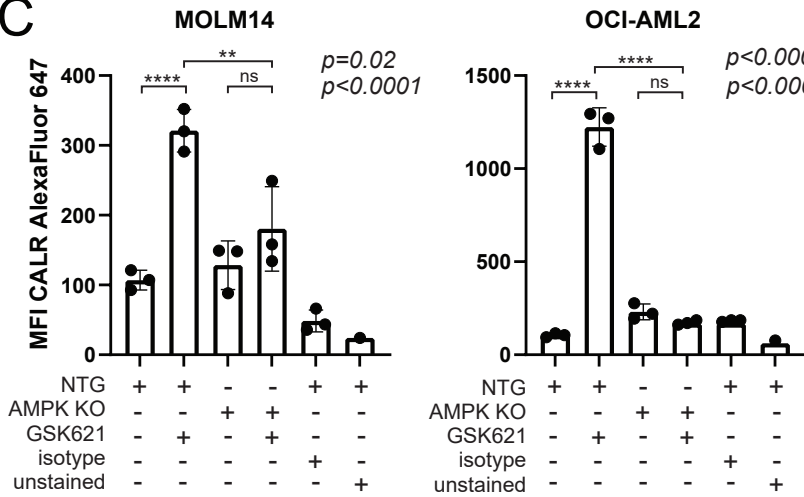
A



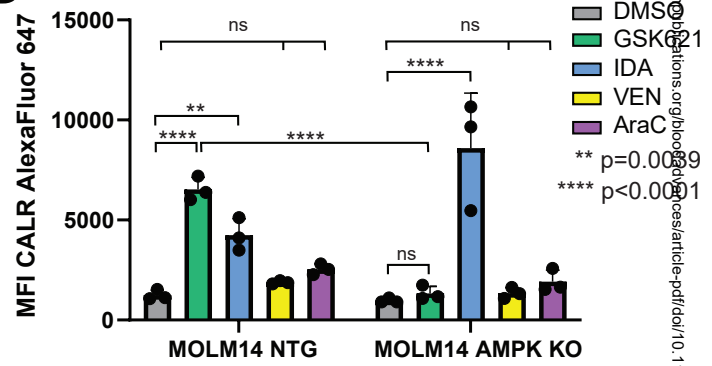
B



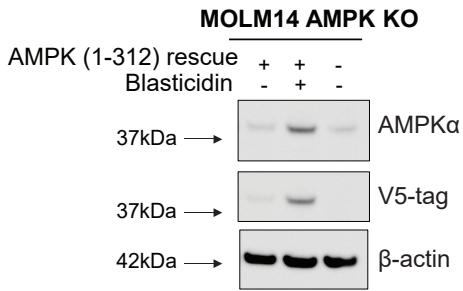
C



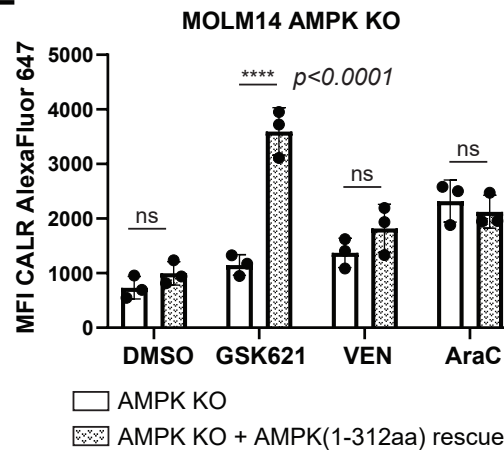
D



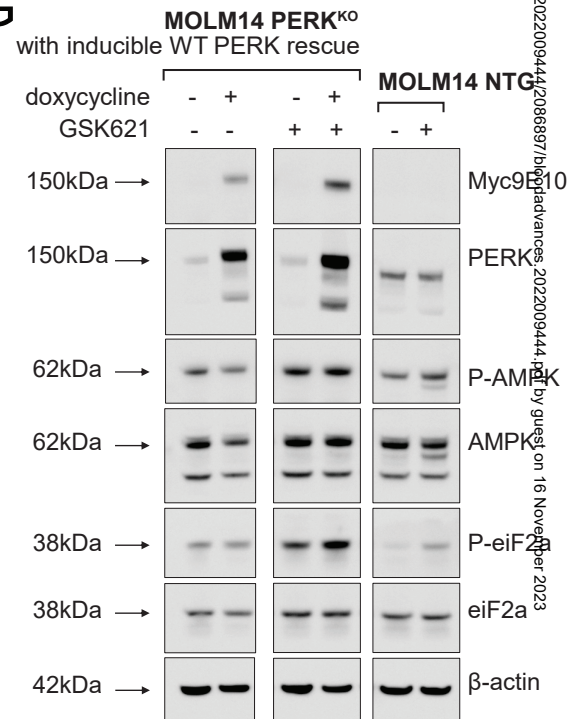
E



F



G



H

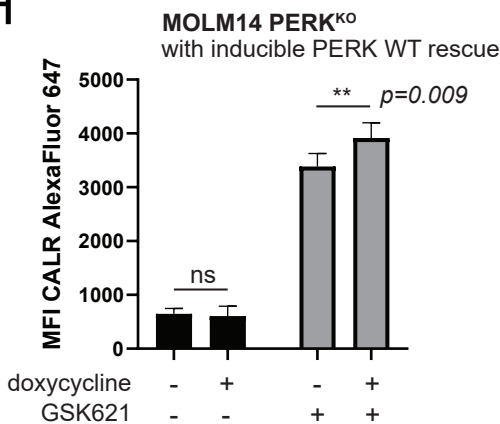
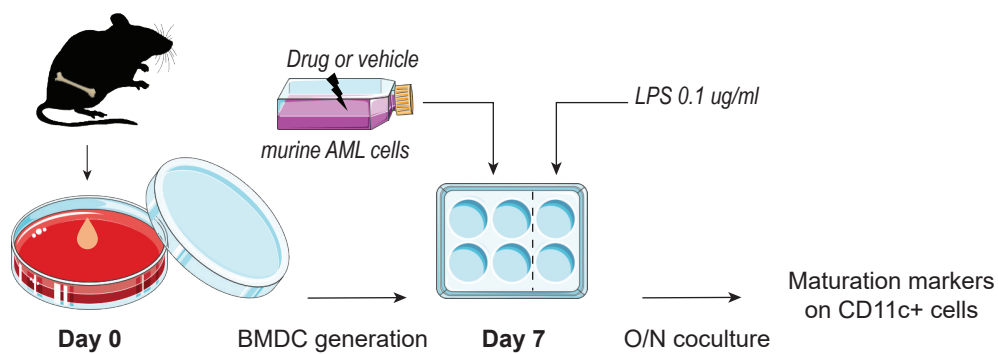
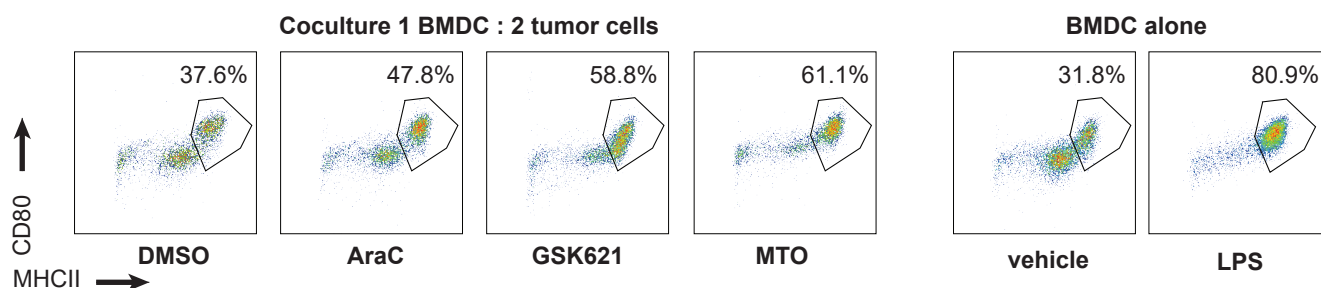


# Figure 3

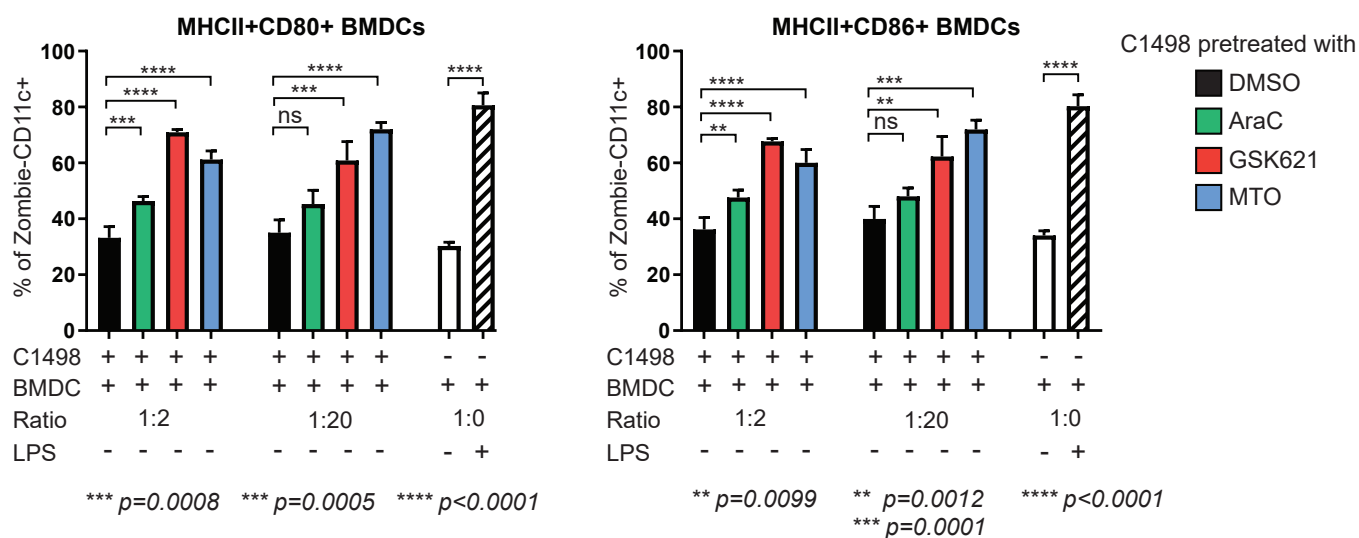
**A**



**B**



**C**



**D**

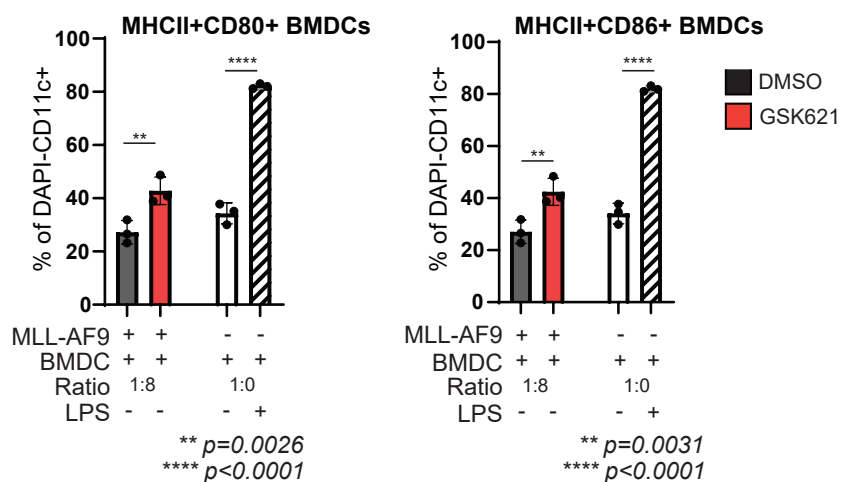


# Figure 4

